

LOW PRESSURE CHEMICAL VAPOR DEPOSITION OF DIFFERENT SILICON NANOSTRUCTURES

M. Ivanda¹, H. Gebavi¹, D. Ristic¹, K. Furic¹, S. Music¹, M. Ristic¹, S. Zonja², P. Biljanovic², O. Gamulin³, M. Balarin³, M. Montagna⁴, M. Ferarri⁵, and G. C. Righini⁶

¹Ruder Bošković Institute, P.O.Box 180, 10002 Zagreb, Croatia

²Faculty for Electrotechnic and Computing, University of Zagreb, Unska 3, 10000 Zagreb

³Medical School, Department of Physics and Biophysics, University of Zagreb, Salata 3b, 10 000, Zagreb, Croatia

⁴Dipartimento di Fisica, Università di Trento and INFN, I-38050 Povo, Trento, Italy

⁵Instituto di Fotonica e Nanotecnologie, CSMFO group, Via Sommarive 14, Trento, I-38050 Trento, Italy

⁶Department of Optoelectronics and Photonics, Nello Carrara Institute of Applied Physics, IFAC - CNR, Via Panciatichi 64, I-50127 Firenze, Italy

Abstract - The low pressure chemical vapor deposition technique was used to deposit different silicon nanostructures by varying the working gas composition and substrate temperature. Silan gas diluted with argon was used to deposit silicon nanocrystals on different temperatures between 650 and 900 °C. The p-doping films of polycrystalline Si films were prepared by using BCl₃ vapor. The SiO₂ nanostructures were deposited by using the mixture of SiH₄+O₂ gasses and, in another case, of SiH₄+N₂O gasses. The structure and optical properties of such nanostructures were examined by Raman and IR spectroscopy, SEM analysis and electrical measurements.

I. INTRODUCTION

The growth of thin films by Low Pressure Chemical Vapour Deposition (LPCVD) is one of the most important techniques for deposition of thin films in modern technology. The reasons of a broad application of the LPCVD method are in the possibility of deposition of different elements and compounds at relatively low temperatures in amorphous and crystalline phase with high degree of uniformity and purity. A simple handling, high reliability of operations, fast deposition, homogeneity of deposited layers and high reproducibility are the basic characteristics the LPCVD method.

The main difference between CVD depositions at low pressure and atmospheric pressure is in ratio of the mass transport velocity and the velocity of reaction on the surface. At atmospheric pressure these quantities are of the same order of magnitude. While the velocity of the mass transport depends mainly on the reactant concentration, diffusion, and thickness of the border layer, the velocity of the

surface reaction depends mainly on the concentration of reactants and temperature. As diffusion of gas is reciprocal to pressure, it will decrease 1000 times if the pressure reduces from atmospheric value to 100 Pa. Now the caring gas is not more necessary, the substrates could approach more closely, and deposited films shows better uniformity and homogeneity.

Investigations concerning polycrystalline films obtained by low pressure chemical vapor deposition were undertaken during the early days of the development of metal-oxide-semiconductor (MOS) electronics and with the first introduction of this material in very large scale integration (VLSI) technology.¹ It was then widely applied in microelectronics and, recently, it is also used as structural material in micromachining applications² and in large area and low cost solar cells.³ Consequently a large effort was performed to understand and optimize its properties. Many detailed studies have concentrated on the mechanisms of growth of the poly-Si films and in particular of the crystallization of amorphous Si upon thermal annealing.^{4,5} When grown by low pressure chemical vapor deposition on silicon oxide films and at low annealing temperature, poly-Si consists of individual grains of uniform size. The crystalline character, which is strongly dependent on both the thickness of the film and the deposition temperature, influences the physical properties of poly-Si. For instance, the thermal conductivity shows a strong dependence of phonon scattering from the structural morphologies, and in particular from the grain size.⁶ In Si based photonics,⁷ poly-Si is a very interesting material due to the diffuse presence in most standard microelectronic processing and due to its large refractive index suitable to produce waveguides⁸ or dielectric stacks.

II. EXPERIMENT

The LPCVD method is most successfully applied in deposition of polysilicon thin films from SiH_4 in the temperature range 600-660 °C and SiO_2 layers from SiH_2Cl_2 at 900 °C. The scheme of the conventional hot-wall horizontal LPCVD reactor is shown on Fig.1. The base of device is a quartz tube placed in a spiral heater. The tube is evacuated on the pressure of 0.1 Pa and heated on to the wanted temperature to 1000 °C. The temperature stability is +/- 1 °C. The deposition starts with entering of the working gas in the tube. The working (dynamical) pressure is 10-200 Pa.

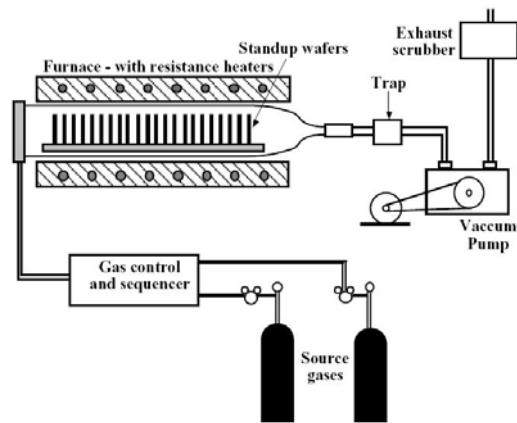


Fig.1. Schematic description of LPCVD device.

The working gas, that regularly consist of the gas for dilution and of the reactive gas, after entering spreads inside the tube and flows above the hot substrates (thin wafers of silicon, quartz or some other material) placed in the quartz holders. The wafers in the tube reactor are radiantly heated by resistive hearing coils surrounding the tube. Because of the depletion effects which reduce gas phase concentration as reactions are consumed by reactions on wafer surfaces are operative in the operator. That is, wafers near the inlet are exposed to higher concentrations of reactant gases. As a result, deposition rate greater on wafers place near the inlet end of the tube. Since the reaction rate increase with increasing temperature, these deposition rate variations can be minimized by linearly increasing temperature via the radiant heating from resistance heated coil that surround the tube. This temperature ramping compensates for the reactant gas depletion and better thickness uniformity is obtained.

The critical factors that influence on thickness uniformity and film content are positions of the substrates, temperature profile in the zone of deposition, reactor geometry, deposition time, working pressure, as well as the quantity and content of all gases or vapors that enter in the reactor. The types of chemical reactions we used here are:

- pyrolysis or thermal decomposition silane: $\text{SiH}_4 \rightarrow \text{Si} + 2\text{H}_2$ - this reaction is activated by the hot surface of substrate and, therefore, appears in the majority of systems;
- p-doping of poly-Si films by using BCl_3 ;
- oxidation of silane with O_2 : $\text{SiH}_4 + 2\text{O}_2 \rightarrow \text{SiO}_2 + 2\text{H}_2\text{O}$;
- oxidation of silane with N_2O : $\text{SiH}_4 + 2\text{N}_2\text{O} \rightarrow \text{SiO}_2 + 2\text{N}_2 + 2\text{H}_2$.

In this experiment the poly-crystalline Si were deposited on 650 nm thick thermal oxide on a (111) oriented silicon substrate with a diameter of 50 mm set at 7 mm from each other. The depositions were carried out by thermal decomposition of 26 % diluted silane in argon at the temperatures 600-900 °C under the silane flow rate of 92 sccm (standard cubic centimeters per minute). The p-doped layers were prepared during silane deposition by flash evaporation of the specified volume of BCl_3 . The concentration of boron atoms was controlled by the number of flashes of BCl_3 . After deposition, the doped polycrystalline silicon films were subjected to wet thermal oxidation treatments under dry water vapor (H_2O) at the temperature of 1100 °C for 1 hour. It is useful to note that we have studied the oxidation kinetics of these films and these results will be published. At this time, after the oxide layers grown on the poly-silicon films are removed with an appropriate solution of hydrofluoric acid prior to electrical characterizations with 4 point resistivity measurements.

For deposition of oxide layers the flow rate ratios $\Phi(\text{O}_2 \text{ or } \text{N}_2\text{O})/\Phi(\text{SiH}_4) = 3.8$ was used. The smaller flow rate ratio $\Phi(\text{N}_2\text{O})/\Phi(\text{SiH}_4) = 1.2$ was used for deposition of silicon reach oxide. The samples were deposited at 748 °C and. The SiO_x films were further thermally annealed at 900 °C, 1000 °C and 1100 °C in air. Upon annealing the decomposition of SiO into SiO_2 and elemental Si takes place. After the decomposition, the excess Si atoms form Si clusters embedded in a SiO_2 matrix. The size of Si clusters is expected to become larger for higher annealing temperatures.

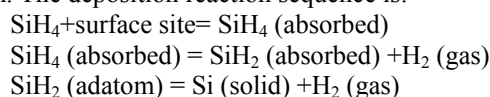
The deposited layers were characterized by Raman scattering, IR absorption spectroscopy and scanning electron microscopy (SEM). The Raman spectra were recorded by the DILOR Z-24 triple monochromator.

III. RESULTS AND DISCUSSION

III.1 Polycrystalline silicon thin films

The silicon deposition processes, in general, are highly complicated and involved several phenomena. In a typical process, the reagent gas molecules are transported near the surface of the substrate by either convection or diffusion. These gas molecules are then adsorbed onto the surface of

the substrate. These adsorbed species migrate on the substrate and decompose resulting in solid and gaseous products. The resulting gaseous product molecules desorbed from the surface and are carried away by either diffusion or convection from the deposition region. The solid product will undergo nucleation and growth resulting in a thin film. The deposition reaction sequence is:



Where the adsorption of the SiH_4 is followed by decomposition to an intermediate compound SiH_2 , then, upon evolution of the remaining hydrogen, the solid film forms, the overall reaction is generally given as: $\text{SiH}_4 \text{ (vapor)} = \text{Si (solid)} + 2\text{H}_2 \text{ (gas)}$. In addition to the above processes, additional complications can arise from the gas-phase decomposition of reagent molecules into many different species.

Poly-Si is generally deposited by pyrolysis (i.e. thermal decomposition) of silane in the temperature range 580-650 °C. The deposition rate shows an exponential dependence on the temperature. Depositions are limited to the 580-650 °C range, since at higher temperatures gas phase reactions occur (leading to rough and loosely adhering films), and below 580 °C the rate is too slow for practical use.

Figure 1 shows the morphology of the surface of poly-crystalline silicon deposited at higher temperatures, but with low silane flow rate of 7 sccm. Within these conditions the deposited films are uniform with small size of crystallites. With increasing the deposition temperature the grain size increases from ~30 nm deposited at 748 °C to ~60 nm deposited at 866 °C. The existence of such small crystallites are also confirmed by Raman scattering where the $\text{TO}(\Gamma)$ phonon bands decreased in frequency and increased in full width at half maximum (FWHM) when the vibrations are confined to the smaller crystal size dimension. Other effects of phonon confinements are observed by the intensity increase of the TA-like phonon band that appears with strong phonon confinement.

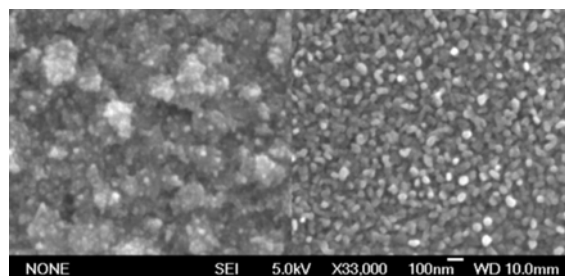


Fig. 2. Poly-crystalline thin films deposited with low silane flow rate of 7 sccm at two different temperatures: left image at 748 °C and right image at 866 °C.

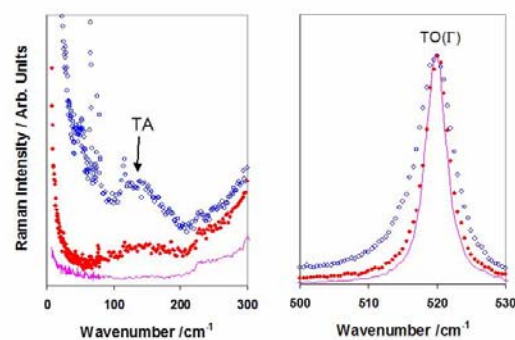


Fig. 3. Raman spectra of poly-crystalline silicon in the range of TA and $\text{TO}(\Gamma)$ phonon bands of the samples deposited at 748 °C (full diamonds) and 866 (open circuits) °C.

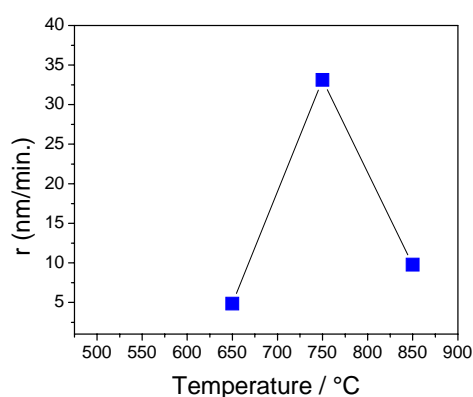


Fig. 4. Growth rate of poly-crystalline silicon films by thermal decomposition of silane.

III. 2. Deposition of p-doped poly-Si films

Morphological differences must reflect some difference on electrical properties. This is in fact what happens for layer resistance and for MOS threshold voltage where these poly-silicon layers are used as gate. Layer sheet resistance of samples deposited at higher pressure show slightly lower values as expected, because of larger grains and hence less percentage of grain boundaries. We present here the results concerning changes in the structural and electrical properties of heavily *in situ* boron-doped polysilicon thin films by the LPCVD method before and after thermal oxidation treatments.

The sheet resistivity, measured using a classical probe set having four probe points, is linear shaped with the dc current passing through two other probes and the voltage measured across the other two inner probes. The average resistivity before and after the thermal oxidation process has been calculated from repeated measurements performed over the surface samples. Particular attention has been taken to keep the four-point

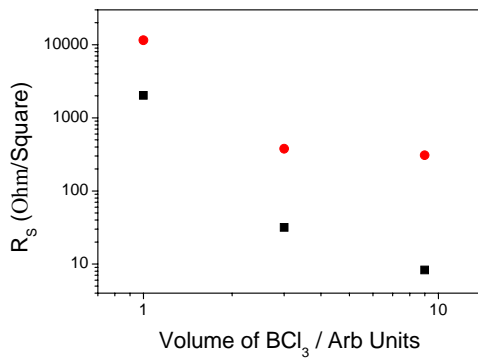


Fig. 5. Sheet resistance of boron doped (circles) and thermal annealed (squares) samples.

probe on the film surface, therefore avoiding point penetration and measuring an average value over a volume under the probe points. Thermal annealing increased the resistivity for more than one order of magnitude of deposited films

III.3. Deposition of SiO₂ films

SiO₂ films continue to be of major importance in micro- and nano-technology^{9,10}. Depending on the growth method SiO₂ films can have different macroscopic features like stresses, density and dielectric strength^{11,12}. All these features are directly related with the way in which Si and O atoms are arranged in the films. IR spectroscopy has been used widely for studying SiO₂ films¹³⁻¹⁹ because of its sensitivity to the Si-O bond.

Figure 6 shows the IR spectra deposited from SiH₄ + O₂ at different temperatures. It was found that the strong peak between 1000 cm⁻¹ and 1100 cm⁻¹ corresponds to the asymmetrical stretching motion of the Si-O-Si bridge. This peak shifts to the higher frequencies (1062-1071 cm⁻¹) and narrow with increasing the deposition temperature. Such effects point out on the structural ordering of deposited layers.

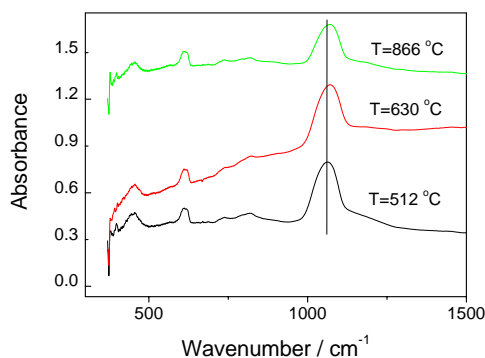


Fig. 6. FTIR spectra of SiO₂ thin films prepared by silane reaction with oxygen.

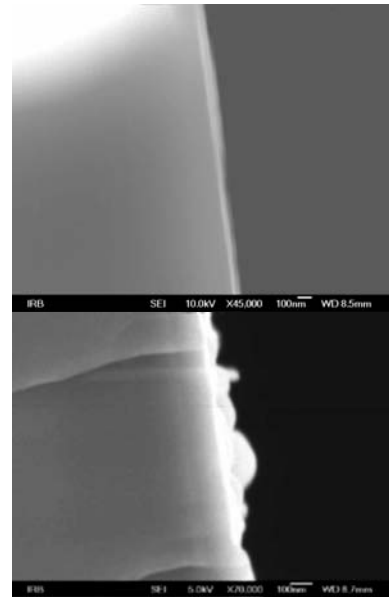


Fig. 7. SEM images of the oxide film prepared by the silane reaction with oxygen at 866 °C (bar represent 100 nm).

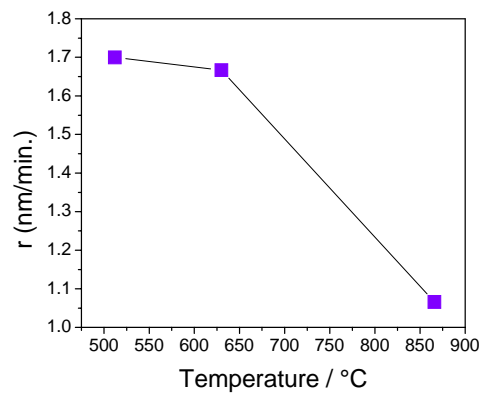


Fig. 8. Growth rate of silicon oxide films deposited from SiH₄ + O₂ in dependence on temperature.

Figure 7 shows the SEM images of the sample deposited at 866 °C. The upper image shows that layer is of homogenous thickness of 100 nm, while the lower image shows that the surface is quite rough. Figure 8 shows that the deposition rate is low and decreases with the temperature. We note here that the layers were obtained with very low gas flow of silane of 7 sccm and of 27 sccm of O₂.

Figure 9 shows the FTIR spectrum of the sample deposited from SiH₄ + N₂O at the temperature of 866 °C and is very similar to the spectrum of the sample prepared with O₂ and deposited at the same temperature (see Fig. 6). The peak position the Si-O-Si bridge vibrations is 1072 cm⁻¹, which is near to thermally grown oxide at ~ 1090 cm⁻¹. This indicates the same ordering of the structure. Contrary the SEM image on Fig. 10. shows that the layer is more porous and inhomogeneous.

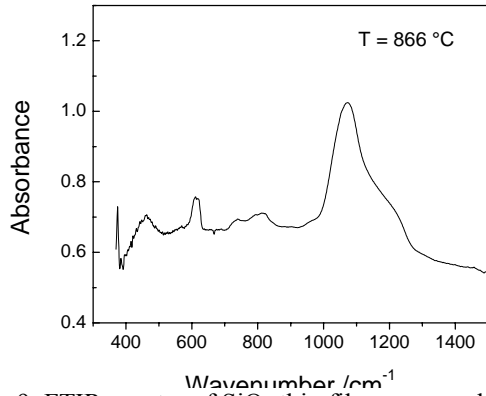


Fig. 9. FTIR spectra of SiO₂ thin films prepared by silane reaction with N₂O.

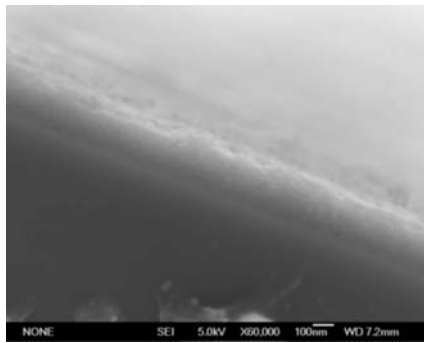


Fig. 10. SEM images of the oxide film prepared by the silane reaction with N₂O at 866 °C (bar represent 100 nm).

The process is activated at the temperatures above 800 °C. The estimated growth rate at 866 °C is 1.14 nm/min which is similar to layers deposited with oxygen.

III. 4. Depositions of silicon rich oxide films

Although crystalline silicon is a key material in the microelectronic industry, its use in optoelectronic applications is hindered because, as an indirect gap semiconductor, its light emission in the visible is inefficient. The observation of strong visible photoluminescence from porous silicon at room temperature²⁰ stimulated substantial activity in the field of preparation of structures comprising silicon nanowires and nanoparticles as well as exploration of their structural and optoelectronic properties.

Silicon nanoparticles in Si-rich silicon oxide films are generally produced by high-temperature annealing in an inert atmosphere. The process is compatible with integrated circuit technology and, moreover, SiO₂ is a robust host that provides good passivation for the Si nanoparticles. In this approach the average nanoparticle size and the

emission properties can be properly tuned either by varying the annealing temperature or by changing the excess silicon content in the deposited films. Figure 11 shows the SiO_x thin films deposited at the temperature of 748 °C with gas flow ratio $\Phi(N_2O)/\Phi(SiH_4) = 1.2$ and thereafter subsequent annealed at the temperatures 900-1100 °C for 1 hour in air. Upon annealing the decomposition of SiO_x into SiO₂ and elemental Si takes place. After decomposition, the excess Si atoms form Si clusters embedded in a SiO₂ matrix. The size of Si clusters is expected to become larger for higher annealing temperatures.

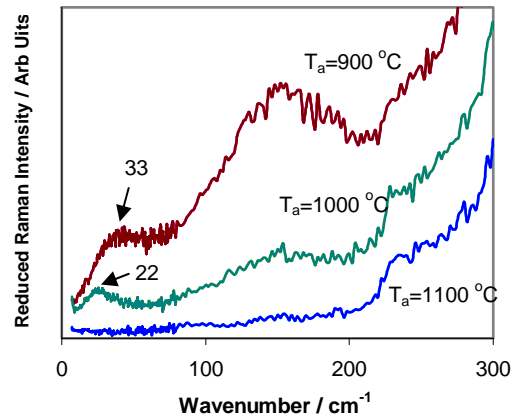


Fig. 11. Low frequency Raman spectra reduced for the Bose-Einstein factor of different nc-Si in SiO_x. The arrow indicate the symmetric vibrational mode of silicon nanoparticles.

Low frequency modes indicated by arrow corresponds to the spherical acoustical modes of silicon nanocrystals. Vibrations of elastic spheres have been studied for a long time by Lamb²¹. The frequency (in wavenumbers) of the symmetric spherical mode is given by²²:

$$v_0 = \frac{S_0 v_L}{cD} \quad (1)$$

where v_0 is the frequency of the surface symmetric modes, D is the diameter of the spherical particle and c is the velocity of light. The constant $S_0=0.76$.²³ The mean value of the longitudinal sound velocities calculated across three crystalline directions is $v_L=8790$ m/s. These parameters when inserted in Eq.(1) give the mean size of silicon nanoparticles from the known frequency of the symmetric spherical mode, i.e. $D=2.29 \times 10^{-7}/v$. In our case the silicon nanocrystals with mean sizes of 6.9 nm and 10.4 nm appeared in the films annealed at 900 and 1000 °C, respectively.

As a conclusion here we have shown that by using LPCVD technique a number of different silicon nanostructures of high quality important for microelectronic and photonic application is possible to prepare with rather simple approach.

ACKNOWLEDGMENTS

This work was supported by the Ministry of Science and Technology of the Republic of Croatia.

REFERENCES

- [1] *Microelectronic Materials and Processes*, edited by R. A. Levy, Kluwer Academic Publishers, London (1989).
- [2] C. A. Zorman and M. Mehregany in *The MEMS Handbook* edited by Mohamed Gad-El-Hak, CRC Press London 2002 Chap 15, pp. 1-9.
- [3] M. J. McCann, K. R. Catchpole, K. J. Weber and A. W. Blakers, *Solar Energy Materials & Solar Cells* **68**, 135 (2001).
- [4] J. L. Batstone, *Philos. Mag. A* **67**, 51 (1993).
- [5] H. Hahn, A. Q. He and A. H. Heuer, *Philos. Mag. A* **82**, 137 (2002).
- [6] S. Uma, A. D. McConnell, M. Asheghi, K. Kurabayashi and K. E. Goodson, *International Journal of Thermophysics*, **22**, 605 (2001).
- [7] *Silicon Photonics*, edited by L. Pavesi and D. Lockwood, Topics in Applied Physics vol. 94, (Springer-Verlag, Berlin 2004).
- [8] A. M. Agarwal, L. Liao, J. S. Foresi, M. R. Black, X. Duan and L. C. Kimerling, *J. Appl. Phys.* **80**, 6120 (1996).
- [9] L.E. Katz In: S.M. Sze, editor. *VLSI Technology*. 2nd ed. McGraw-Hill International Editions; 1988.
- [10] R.B. Fair In: C.Y. Chang, S.M. Sze, editors. *ULSI technology*. McGraw-Hill International Editions; 1996.
- [11] W.A. Pliskin, H.S. Lehman, *J. Electrochem. Soc.* **112**, 1013. (1965).
- [12] I.W. Boyd, J.I.B. Wilson, *J. Appl. Phys.* **53**, 4166 (1982).
- [13] PG Pai, SS Chao, Y Takagi, G. J Lucovsky, *Vac. Sci. Technol. A* **4**, 689 (1986) .
- [14] G. Lucovsky, J.T. Fitch, D.V. Tsu, S.S. Kim, *J Vac. Sci. Technol. A* **7**, 1136 (1989).
- [15] W. Calleja, C. Falcony, A. Torres, M. Aceves, R. Osorio, *Thin Solid Films* **270**, 114 (1995).
- [16] C. Falcony, W. Calleja, M. Aceves, J. M. Siqueiros, R. Machorro, L. Cotta-Araiza et al. *J. Electrochem. Soc.* **144**, 379 (1997).
- [17] D.V. Tsu, *J. Vac. Sci. Technol. B* **18**, 1796 (2000).
- [18] M. K. Weldon, K. T. Queeney, Y. J. Chabal, B. B. Stefanov, K. Raghavachari, *J. Vac. Sci. Technol. B* **17**, 1795 (1999).
- [19] Y.J. Chabal, K. Raghavachari, X. Zhang, E. Garfunkel, *Phys. Rev. B* **66**, 161315(R) (2002).
- [20] L. T. Canham, *Appl. Phys. Lett.* **57**, 1046 (1990).
- [21] H. Lamb, *Proc. Math. Soc. Lond.* **13** 187 (1882).
- [22] M. Ivanda, K. Babocsi, C. Dem, M. Schmitt, M. Montagna, W. Kiefer, *Phys. Rev. B* **67**, 235329 (2003).
- [23] M. Ivanda, A. Hohl, M. Montagna, G. Mariotto, M. Ferrari, Z. Crnjak Orel, A. Turković, and K. Furić, *J. Raman Spectroscopy* **37**, 161-165 (2006).